From: MECHANICS OF SHEET METAL FORMING (1978)
Edited by Donald P. Koistinen and Neng-Ming Wang
Book available from: Plenum Publishing Corporation
227 West 17th Street, New York, N Y. 10011

SHEET NECKING—I. VALIDITY OF PLANE STRESS ASSUMPTIONS OF THE LONG-WAVELENGTH APPROXIMATION*

J. W. HUTCHINSON

Harvard University, Cambridge, Massachusetts

K. W. NEALE

Université de Sherbrooke, Sherbrooke, Quebec, Canada

A. NEEDLEMAN

Brown University, Providence, Rhode Island

ABSTRACT

Two special solutions are used to illustrate the errors involved in the analysis of sheet necking from invoking plane stress assumptions. The first is an exact solution for the growth-rate of a small amplitude, sinusoidal thickness variation in a sheet of material characterized by $\dot{\epsilon} = \alpha\sigma^n$ in simple tension. The plane stress assumptions become accurate when the ratio of variation wavelength to average thickness exceeds four and otherwise lead to overestimates of the actual growth-rate. When this same ratio is approximately unity the relative size of the thickness variation decays with increasing deformation—an effect not predicted by a plane stress analysis. The second special solution is obtained using a perturbation expansion with the nonlinear long-wavelength solution (i.e., the plane stress solution) as the lowest order contribution. In this way explicit corrections to the plane stress solution are obtained. Selected comparisons with fully nonlinear finite element calculations are made.

INTRODUCTION

The list of variables and issues thought to be important in the analysis of necking failures in thin sheet metals has almost reached perplexing proportions.

* *The material in this three-part paper was presented orally in Session II under the title "Constitutive Relations for Sheet Metal" and Session IV under the title "Sheet Necking: Influence of Constitutive Theory and Strain-Rate Dependence."*

References p. 126.

Included are not only strain hardening and plastic anisotropy characteristics but also strain-rate sensitivity, choice of plastic constitutive law, bifurcation analysis vs. imperfection growth analysis, and microscopic fracturing and void growth. In the three parts of this paper an attempt will be made to give a unified examination of the role of a number of these in the analysis of sheet metal necking.

Part I deals with the adequacy of the plane stress assumptions often invoked in the analysis of sheet necking. We will refer to a solution based on these assumptions as the long-wavelength approximation, and we obtain some indication of the range of validity of this approximation by way of two special solutions and some fully nonlinear finite element calculations.

Choice of constitutive law will be central to Parts II and III with time-independent material behavior discussed in II and rate-dependent behavior featured in III. In II a bifurcation analysis of localized necking will be given side by side with a long-wavelength analysis of the growth of initial nonuniformities of the type introduced by Marciniak and Kuczyński [1]. Differences in forming limit diagrams computed using a standard flow (incremental) theory of plasticity on the one hand and a deformation theory on the other will be noted. These differences are large when both principal in-plane strains are positive. There is reason to doubt whether a standard flow theory can be used to analyze localized necking in sheet metals. This is clearly an important issue since large scale numerical programs are currently being developed to cope with complications associated with particular sheet forming operations. It is essential that limitations of competing constitutive laws be well understood.

The effect of strain-rate dependence on constitutive behavior is incorporated in III in a simple and straightforward manner. The influence of small amounts of rate-sensitivity on the forming limit diagrams is emphasized.

PLANE STRESS ASSUMPTIONS OF THE LONG-WAVELENGTH APPROXIMATION

In Part I attention will be restricted to in-plane plane strain deformations of a sheet subject to a tensile load per unit length P acting in the x_1-direction as shown in Fig. 1. The surface of the sheet at any instant of time t and position x_1 is symmetrically disposed about its midplane at $x_3 = 0$ according to $x_3 = \pm h(x_1, t)/2$. Under in-plane plane strain all quantities are independent of x_2 and no straining in the x_2-direction is permitted. In the plane stress approximation only the stress components σ_{11} and σ_{22} are assumed to be nonzero and these are taken to be uniform over each section $x_1 = \text{const}$. For each value of x_1 equilibrium requires

$$P = \sigma_{11} h \tag{1}$$

Nonzero strain-rates are $\dot{\epsilon}_{11}$ and $\dot{\epsilon}_{33}$ and these are also uniform over each section. These, together with (1), the constitutive law and $\dot{\epsilon}_{22} = 0$, can be used to eliminate σ_{22} and to formulate equations governing the evolution of the thickness variation.

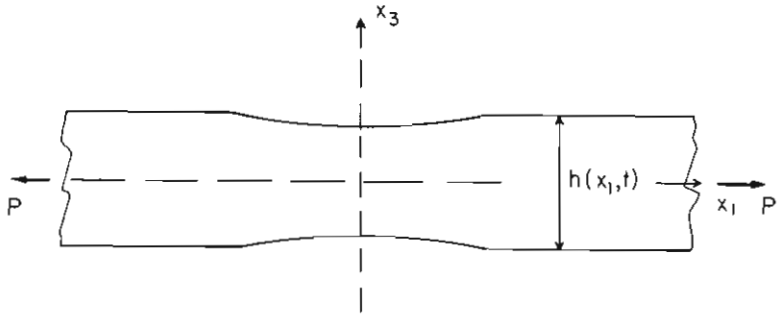

Fig. 1. Sheet geometry.

In what follows, we give a detailed assessment of the consequences of the plane stress assumptions using two special solutions: (1) a linearized solution for the growth-rate of thickness variations of arbitrary wavelength, and (2) a perturbation solution valid for moderately-long-wavelength variations. For this purpose we consider an incompressible, strain-rate dependent material characterized in simple tension by the pure power law

$$\dot{\epsilon} = \alpha \sigma^n \tag{2}$$

where σ is the true stress and $\dot{\epsilon}$ is the natural strain-rate. Revealing results can be obtained using analytic methods for this relatively simple class of materials since the prior deformation history in any problem appears only through the current geometry. Such results are applicable to super plastic behavior and to materials undergoing power law creep. While these results can not be expected to apply directly to problems involving more complex material behavior, they should serve to illustrate some of the most important points at issue in the validity of the plane stress assumptions.

With s_{ij} as the deviator of the true stress σ_{ij} and σ_e as the effective stress, the Eulerian strain-rate under a general stress state is taken to be

$$\dot{\epsilon}_{ij} = \tfrac{3}{2}\alpha \sigma_e^{n-1} s_{ij}, \qquad \sigma_e = (3 s_{ij} s_{ij}/2)^{1/2} \tag{3}$$

which generalizes (2).

In the plane stress approximation the strain-rates at each position x_1 can readily be found in terms of the current thickness variation $h(x, t)$ as

$$\dot{\epsilon}_{11} = -\dot{\epsilon}_{33} = (\sqrt{3}/2)\alpha[\sqrt{3}P/(2h)]^n \tag{4}$$

The corresponding (convected) rate of change of the thickness of the material element currently at x_1 is given by

$$\dot{h} \equiv \frac{\partial h}{\partial t} + v_1 \frac{\partial h}{\partial x_1} = \dot{\epsilon}_{33} h = -\dot{\epsilon}_{11} h \tag{5}$$

where $v_1(x_1)$ is the velocity in the x_1-direction.

References p. 126.

LINEARIZED ANALYSIS FOR SMALL NONUNIFORMITIES OF ARBITRARY WAVELENGTH

Consider a sheet of material (3) under in-plane plane strain conditions and subject to a load per unit length P. Let $h_0(t)$ denote the evolving thickness of a perfect sheet with no variation in thickness. Equations (4) and (5) involve no approximation for the perfect sheet so that

$$-\dot{h}_0/h_0 = \dot{\epsilon}_{11} = -\dot{\epsilon}_{33} = \dot{\epsilon}_0 \equiv (\sqrt{3}/2)\alpha[\sqrt{3}P/(2h_0)]^n \tag{6}$$

where ϵ_0 is the strain-rate in the perfect sheet. We also consider a nonuniform sheet characterized at the current instant by a symmetric thickness variation

$$h = h_0[1 - \xi \cos(2\pi x_1/l)] \tag{7}$$

For $|\xi| \ll 1$, an exact linearized solution for the strain-rate and rate of change of the nonuniformity can be obtained along lines similar to those given for the analogous problem for a circular bar in [2, 3]. Velocity fields (v_1, v_3) can be expressed in terms of a velocity potential $\Phi(x_1, x_3)$ by

$$v_1 = \Phi_{,x_3}, \qquad v_3 = -\Phi_{,x_1} \tag{8}$$

The solution for Φ is simpler than that for the circular bar given in detail in [2], and therefore we will proceed directly to give the end result. Let ζ be the first quadrant root of

$$\zeta^2 = \left(1 - \frac{2}{n}\right) + i\sqrt{1 - \left(1 - \frac{2}{n}\right)^2} \quad (i \equiv \sqrt{-1}) \tag{9}$$

and let

$$q = \pi h_0/l \tag{10}$$

With terms of order ξ^2 neglected, the solution for Φ is

$$\Phi = \dot{\epsilon}_0 x_1 x_3 + \xi \frac{\dot{\epsilon}_0 l h_0}{\pi} \mathrm{Re}\left[c \sin\left(\frac{2\zeta q x_3}{h_0}\right)\right] \sin\left(\frac{2\pi x_1}{l}\right) \tag{11}$$

where Re denotes the real part and c is a complex constant satisfying

$$\left.\begin{aligned} \mathrm{Re}[c(1 - \zeta^2)\sin(\zeta q)] &= 1 \\ \mathrm{Re}[c\zeta(1 - \zeta^2 - 4/n)\cos(\zeta q)] &= 0 \end{aligned}\right\} \tag{12}$$

Let $\Delta h(x_1, t) = h(x_1, t) - h_0(t)$ be the nonuniformity in thickness and let

$$a = \Delta h(x_1, t)/h_0(t) \tag{13}$$

measure the size of the nonuniformity relative to the evolving thickness of the perfect sheet. At the current instant, therefore,

$$a = -\xi \cos(2\pi x_1/l) \tag{14}$$

From the above linearized solution the convected rate of a can be found to be

$$\dot{a} = -\xi n \dot{\epsilon}_0 G(n, q) \cos(2\pi x_1/l) \tag{15}$$

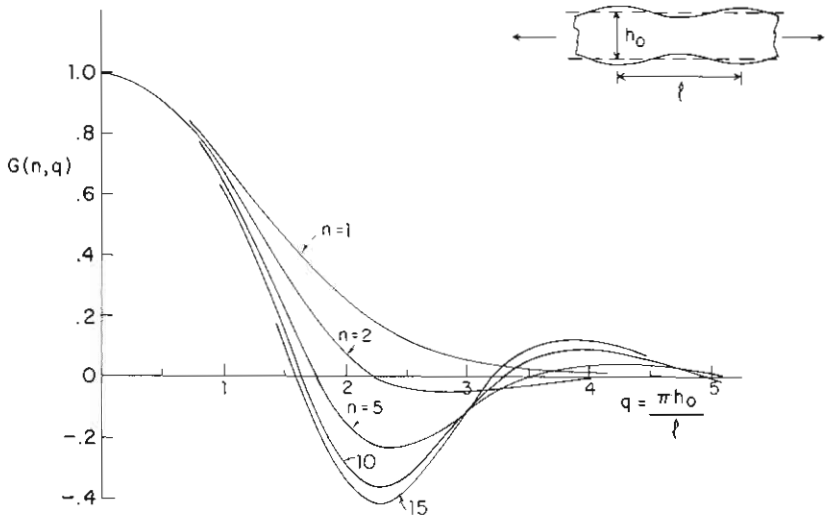

Fig. 2. Values of $G(n, q)$ in Equation (16).

or, from (14),

$$\dot{a} = n\dot{\epsilon}_0 a G(n, q) \tag{16}$$

where

$$G(n, q) = (4/n)\,\mathrm{Re}[c \sin(\zeta q)] \tag{17}$$

Curves of G vs. q for fixed values of n have been calculated numerically from (17) and (12) and are shown in Fig. 2. In the long-wavelength limit (i.e., $q \to 0$) it is seen that $G = 1$ so that

$$\dot{a} = n\dot{\epsilon}_0 a \tag{18}$$

This simple result can be obtained directly from an analysis using the plane stress assumptions of the previous section. Henceforth we will refer to the solution based on the plane stress assumptions as the long-wavelength approximation. From Fig. 2 it can be noted that (18) is reasonably accurate for values of l/h_0 greater than about 4. For nonuniformities shorter than this the long-wavelength result (18) *overestimates* the rate of growth of the nonuniformity. More surprising is the prediction that, for wavelength ratios in the approximate range $1 < l/h_0 < 2$, G is negative and the relative size of the nonuniformity actually decays, except for $n = 1$.*

A similar phenomenon has been observed by Appleby and Richmond [4] in a

* *The analogous equation for round bars in* [3] *for the growth of the relative size of the nonuniformity of cross-sectional area also takes the form (16). For the round bar, however,* G *is never negative and thus decay of the nonuniformity as measured by its* relative *size does not occur for any wavelengths. In this case the long-wavelength analysis is accurate for nonuniformity wavelengths greater than about three diameters. For shorter wavelengths it also overestimates the growth-rate*

numerical study of the growth of sinusoidal geometric imperfections of various wavelengths in sheets of time-independent elastic-plastic materials under similar in-plane plane strain conditions. Using the absolute size of the nonuniformity, Δh, as their measure, they find that Δh grows for $l/h_0 > 2$ and that Δh diminishes for $l/h_0 < 2$. Furthermore, they find that the "most stability", i.e., fastest rate of decay in Δh, occurred for l/h_0 around unity. This leads them to make the intriguing suggestion that, if controlled favorable nonuniformities are deliberately imposed on a sheet, its ductility might be enhanced. The present equation (16) for $\dot{a}$ can readily be converted to an equation for $\Delta\dot{h}$ using $\dot{a} = \Delta\dot{h}/h_0 + a\dot{\epsilon}_0$, which follows from (13) and (6). Thus (16) transforms to

$$\Delta\dot{h} = (n-1)F(n, q)\dot{\epsilon}_0\Delta h \tag{19}$$

where $F = (nG - 1)/(n - 1)$. In this equation F has been defined such that in the long-wavelength limit, $q \to 0$, $F = 1$. The calculations of Appleby and Richmond were carried out for a material with a strain hardening exponent between $n = 4$ and $n = 5$. Using the curve for $n = 5$ in Fig. 2, we first note that $F = 0$ at a value of $q \cong 1.5$ which corresponds very closely to the transition value $l/h_0 \cong 2$ for the sign of $\Delta\dot{h}$ found by Appleby and Richmond. Secondly, the most negative value of F occurs when $dF/dq = dG/dq = 0$ at about $q = 2.5$ for $n = 5$. This value, too, is not far from the value $l/h_0 \cong 1$ found by Appleby and Richmond for wavelength giving the maximum rate of decay. Thus we can note that some quantitative details as well as qualitative ones, for the simple time-dependent material (3), apply to more complicated time-independent materials.

LOWEST ORDER CORRECTIONS TO THE NONLINEAR LONG-WAVELENGTH APPROXIMATION

In this section a perturbation method is used to show that the long-wavelength solution obtained by invoking the plane stress assumptions is an exact solution in an appropriate limiting sense. In addition, the lowest order corrections to this solution are produced. In particular, deviations of the stresses and strain-rates from the values of the long-wavelength solution will be given. We continue to consider a sheet of power law material characterized by (3) under in-plane plane strain conditions. Now, however, it is not assumed that the variation in thickness is necessarily small and thus full nonlinear behavior is treated.

The starting point in the analysis is the introduction of the perturbation parameter β. Consider a family of similarly shaped, symmetric thickness variations $h(\beta x_1)$ which differ from one another only in scaling in the x_1-direction depending on β. One such variation is depicted in Fig. 3. As $\beta \to 0$ the characteristic wavelength of the variation becomes large compared to the average thickness of the sheet, and it is in this limiting sense that the long-wavelength solution becomes increasingly accurate, as will be shown. For convenience let $z \equiv x_3$ and introduce a scaled variable

$$X = \beta x_1$$

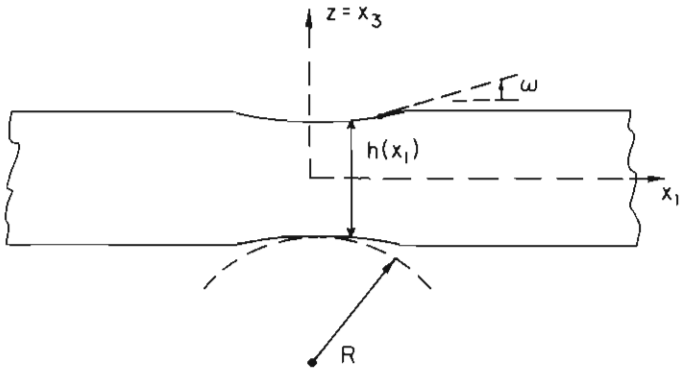

Fig. 3. Sheet geometry.

With

$$\sigma(X) = P/h(X) \tag{20}$$

and

$$\dot{\epsilon}(X) = (\sqrt{3}/2)\alpha[\sqrt{3}\sigma(X)/2]^n \tag{21}$$

the nonzero stresses and strain-rates of the previous nonlinear long-wavelength solution are given by

$$\left.\begin{aligned} \sigma_{11} &= 2\sigma_{22} = 2\sigma_e/\sqrt{3} = \sigma(X) \\ \dot{\epsilon}_{11} &= -\dot{\epsilon}_{33} = \dot{\epsilon}(X) \end{aligned}\right\} \tag{22}$$

Field equations for the fully nonlinear plane strain problem are given below using X and z as independent variables. Equilibrium requires

$$\left.\begin{aligned} \beta\sigma_{11,X} + \sigma_{13,z} &= 0 \\ \beta\sigma_{13,X} + \sigma_{33,z} &= 0 \end{aligned}\right\} \tag{23}$$

Velocities are related to the velocity potential by

$$v_1 = \Phi_{,z} \quad \text{and} \quad v_3 = -\beta\Phi_{,X} \tag{24}$$

Strain-rates are given by

$$\dot{\epsilon}_{11} = \beta v_{1,X}, \quad \dot{\epsilon}_{33} = v_{3,z}, \quad 2\dot{\epsilon}_{13} = v_{1,z} + \beta v_{3,X} \tag{25}$$

Strain-rates and stresses are related through (3). Under the present in-plane plane strain conditions $\sigma_{22} = (\sigma_{11} + \sigma_{33})/2$ so that

$$s_{11} = -s_{33} = (\sigma_{11} - \sigma_{33})/2 \tag{26}$$

and

$$\sigma_e = [3(\sigma_{11} - \sigma_{33})^2/4 + 3\sigma_{13}^2]^{1/2} \tag{27}$$

References p. 126.

Traction-free conditions along $y = h(X)/2$ are

$$\left.\begin{aligned} -\sigma_{11}\sin\omega + \sigma_{13}\cos\omega &= 0 \\ -\sigma_{13}\sin\omega + \sigma_{33}\cos\omega &= 0 \end{aligned}\right\} \tag{28}$$

where

$$\tan\omega = \beta h'(X)/2$$

Here and throughout the remainder of Part I

$$(\quad)' = \frac{d(\quad)}{dX}$$

For future use, expansions of the boundary conditions in powers of β are

$$-\sigma_{11}\beta h'/2 + \sigma_{13}(1 - \beta^2 h'^2/8) + O(\beta^3) = 0 \tag{29}$$

$$-\sigma_{13}\beta h'/2 + \sigma_{33}(1 - \beta^2 h'^2/8) + O(\beta^3) = 0 \tag{30}$$

These equations are supplemented by the condition that all fields must be symmetric about $z = 0$. Overall equilibrium with the applied force per unit length P requires that for every X

$$\int_{-h/2}^{h/2} \sigma_{11}\, dz = P \tag{31}$$

We expand all quantities in a regular perturbation expansion in powers of β, anticipating that the zeroth order terms in the expansion are given by the long-wavelength solution (22). The expansion is of the form

$$\left.\begin{aligned} \sigma_{11} &= \sigma(X) + \beta\sigma_{11}^{(1)} + \beta^2\sigma_{11}^{(2)} + \cdots \\ \sigma_{33} &= \beta\sigma_{33}^{(1)} + \beta^2\sigma_{33}^{(2)} + \cdots \\ \sigma_{13} &= \beta\sigma_{13}^{(1)} + \beta^2\sigma_{13}^{(2)} + \cdots \end{aligned}\right\} \tag{32}$$

$$\left.\begin{aligned} \dot\epsilon_{11} &= -\dot\epsilon_{33} = \dot\epsilon(X) + \beta\dot\epsilon_{11}^{(1)} + \beta^2\dot\epsilon_{11}^{(2)} + \cdots \\ \dot\epsilon_{13} &= \dot\epsilon_{13}^{(0)} + \beta\dot\epsilon_{13}^{(1)} + \beta^2\dot\epsilon_{13}^{(2)} + \cdots \end{aligned}\right\} \tag{33}$$

$$\left.\begin{aligned} \Phi &= \beta^{-1} z \int^X \dot\epsilon(\bar X)\, d\bar X + \Phi^{(0)} + \beta\Phi^{(1)} + \beta^2\Phi^{(2)} + \cdots \\ v_1 &= \beta^{-1} \int^X \dot\epsilon(\bar X)\, d\bar X + v_1^{(0)} + \beta v_1^{(1)} + \beta^2 v_1^{(2)} + \cdots \\ v_3 &= -z\dot\epsilon(X) + \beta v_3^{(1)} + \beta^2 v_3^{(2)} + \cdots \end{aligned}\right\} \tag{34}$$

The terms in the expansions are assumed to be functions of X and z. The term $\dot\epsilon_{13}^{(0)}$ is zero but the development which follows is clearer if it is carried along for the moment.

by (38_1) and (42),

$$\sigma_{11}^{(1)} = \sigma f_1'/(n\dot{\epsilon})$$

But imposition of (36) implies $f_1' = 0$ and thus $\sigma_{11}^{(1)} = 0$. Without loss in generality we may take $f_1 = 0$.

Repetition of the above procedure for the next higher order terms in each of the equations leads to

$$\left.\begin{aligned} \sigma_{13}^{(2)} &= 0, \qquad \sigma_{33}^{(2)} = \sigma h[h'' - 4(h^{-2}h')'z^2]/8 \\ \Phi^{(2)} &= f_4(X)z, \qquad \dot{\epsilon}_{13}^{(2)} = 0, \qquad \dot{\epsilon}_{11}^{(2)} = f_3' + (4 - n)(\dot{\epsilon}h'/h)'z^2/2 \end{aligned}\right\} \tag{44}$$

Furthermore, (44_2) together with (38_2) and (36) give

$$f_3' = (n\dot{\epsilon}/24)[(5 - n)h'^2 - (1 + 4/n)hh''] \tag{45}$$

and

$$\sigma_{11}^{(2)} = (\sigma/24)[1 - 12(z/h)^2][(5 - n)h'^2 + 2(1 - 2/n)hh''] \tag{46}$$

This completes the solution for the stresses and strain-rates up to and including terms of order β^2.

We now examine in some detail the distribution of stress and strain-rate across the minimum section of the neck. Take the minimum section to lie at $X = x_1 = 0$, as depicted in Fig. 3, so that $h'(0) = 0$. With h, h'', σ, etc., now denoting values at the minimum section, the above results specialize to

$$\left.\begin{aligned} \sigma_{11} &= \sigma\{1 + (\beta^2/(12n))(n - 2)hh''[1 - 12(z/h)^2]\} \\ \sigma_{33} &= \sigma(\beta^2/8)hh''[1 - 4(z/h)^2] \\ \sigma_e &= (\sqrt{3}\sigma/2)\{1 - (\beta^2/(24n))hh''[n + 4 + 12(n - 4)(z/h)^2]\} \\ \dot{\epsilon}_{11} &= \dot{\epsilon}\{1 - (\beta^2/24)hh''[n + 4 + 12(n - 4)(z/h)^2]\} \end{aligned}\right\} \tag{47}$$

to order β^2 with $\sigma_{13} = \dot{\epsilon}_{13} = 0$. For $n = 4$, σ_e and $\dot{\epsilon}_{11}$ are uniform across the minimum section of the neck to this order. Furthermore, for $n = 4$, or at $z = 0$ for any n, σ_e and $\dot{\epsilon}_{11}$ are diminished below their respective long-wavelength values by an amount proportional to $\beta^2 hh''$. Let R be the radius of curvature of the surface of the sheet at the neck minimum which is given by

$$\frac{1}{R} = \frac{1}{2}\frac{d^2h}{dx_1^2} = \frac{1}{2}\beta^2 h'' \tag{48}$$

Noting that the combination $\beta^2 hh''$ equals $2h/R$, we can therefore write to order h/R

$$\sigma_e = \frac{\sqrt{3}}{2}\sigma\left\{1 - \frac{h}{R}\left[\frac{n + 4}{12n} + \frac{(n - 4)}{n}\left(\frac{z}{h}\right)^2\right]\right\} \tag{49}$$

$$\dot{\epsilon}_{11} = \dot{\epsilon}\left\{1 - \frac{h}{R}\left[\frac{n + 4}{12} + (n - 4)\left(\frac{z}{h}\right)^2\right]\right\} \tag{50}$$

The hydrostatic tension distribution across the neck minimum is given by

$$\frac{1}{3}\sigma_{pp} = \frac{1}{2}\sigma\left\{1 + \frac{h}{R}\left[\frac{5n-4}{12n} - \frac{(3n-4)}{n}\left(\frac{z}{h}\right)^2\right]\right\} \tag{51}$$

To draw comparison with Bridgman's [5] formulas for the stress distribution at a plane strain neck in a sheet of time-independent plastic material, we use (47) and (48) to determine the ratios

$$\begin{aligned}\frac{\sigma_{11}}{(2\sigma_e/\sqrt{3})} &= 1 + \frac{1}{4}\frac{h}{R}\left[1 - 4\left(\frac{z}{h}\right)^2\right] \\ \frac{\sigma_{33}}{(2\sigma_e/\sqrt{3})} &= \frac{1}{4}\frac{h}{R}\left[1 - 4\left(\frac{z}{h}\right)^2\right]\end{aligned} \tag{52}$$

These ratios, which are independent of n, are identical to the analogous expressions obtained from Bridgman's formulas when his expressions are expanded out up to terms of order h/R. Bridgman's starting point is the assumption ϵ_{11} and σ_e are uniform across the neck. For the present time-dependent power law material this is precisely true only when $n = 4$, to order h/R. For $n < 4$ the effective stress and the strain-rate are largest at the surface of the sheet, while for $n > 4$ they are largest at the midplane. The hydrostatic tension is maximum at the midplane if $n > 4/3$.

COMPARISONS WITH NUMERICAL SOLUTIONS

Let $\dot{\epsilon}_A$ and $\dot{\epsilon}_B$ be the strain-rates as predicted by the long-wavelength analysis at any two material cross-sections with h_A and h_B as the current thicknesses. From (4) any two such strain-rates are related by

$$\dot{\epsilon}_A h_A{}^n = \dot{\epsilon}_B h_B{}^n \tag{53}$$

Since

$$\dot{h}_A = -\dot{\epsilon}_A h_A, \qquad \dot{h}_B = -\dot{\epsilon}_B h_B \tag{54}$$

the respective true strains can be written in terms of the current thickness and the initial thicknesses, $h_A{}^0$ and $h_B{}^0$, as

$$\epsilon_A = -\ln(h_A/h_A{}^0), \qquad \epsilon_B = -\ln(h_B/h_B{}^0) \tag{55}$$

Equations (53) and (55) can be combined and integrated to give

$$1 - e^{-n\epsilon_A} = (h_B{}^0/h_A{}^0)^n(1 - e^{-n\epsilon_B}) \tag{56}$$

which provides a relation between the strains at any two cross-sections independent of the loading history.

To make a direct comparison with the long-wavelength result (56) and some full finite element calculations, we consider a sheet whose initial thickness variation is given by (7). The finite element procedure has been specially tailored to

References p. 126.

deal with the class of materials (3). Incompressible plane strain elements [6] have been designed for the purpose and a Newton-Raphson procedure is used to solve the nonlinear equations at each time step. Periodicity and symmetry in the x_1-direction permit the use of a finite element grid over just one half-wavelength of the current geometry, which is updated each time step. A zero shear stress σ_{13} and a uniform velocity v_1 over each end of the half-wavelength sector can be imposed as boundary conditions. From the homogeneity of the constitutive law (3), it can be shown that the simple property noted in conjunction with (56) generalizes such that the ratio of any strain component at one point, say ϵ_{11}^A, to any component at another point, say ϵ_{11}^B, is independent of the load history $P(t)$. Thus the results in Figs. 4 and 5 for ϵ_A/ϵ_B vs. ϵ_B, comparing the long-wavelength result (56) and the finite element results, do not depend on load history when presented in this manner.

The initial amplitude in (7) for the calculated results in Fig. 4 is $\xi = .01$ and $n = 5$. For the long-wavelength curve ϵ_A is the strain at the minimum section ($x = 0$) and ϵ_B is the strain at the thickest section ($x = l/2$). Thus, from (7), the

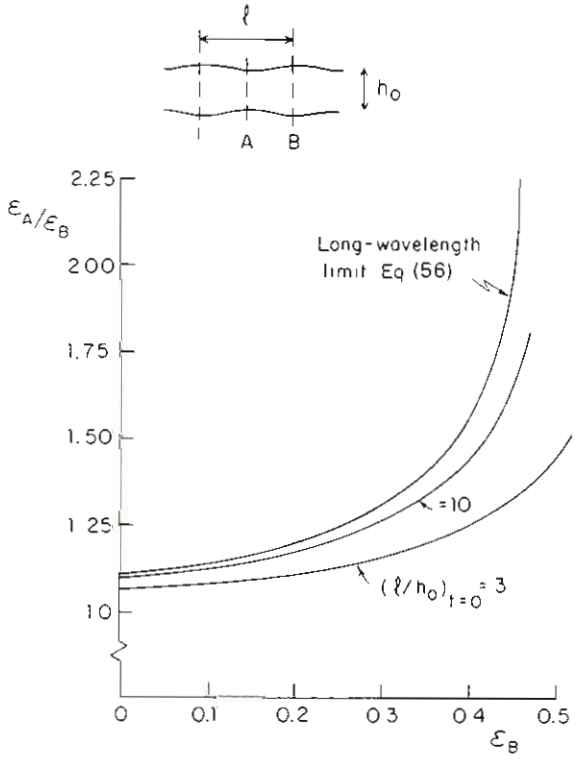

Fig. 4. Strains at the thinnest and thickest sections of the sheet for two initial wavelength to thickness ratios compared with long-wavelength prediction. (Initial amplitude $\xi = .01$; $n = 5$).

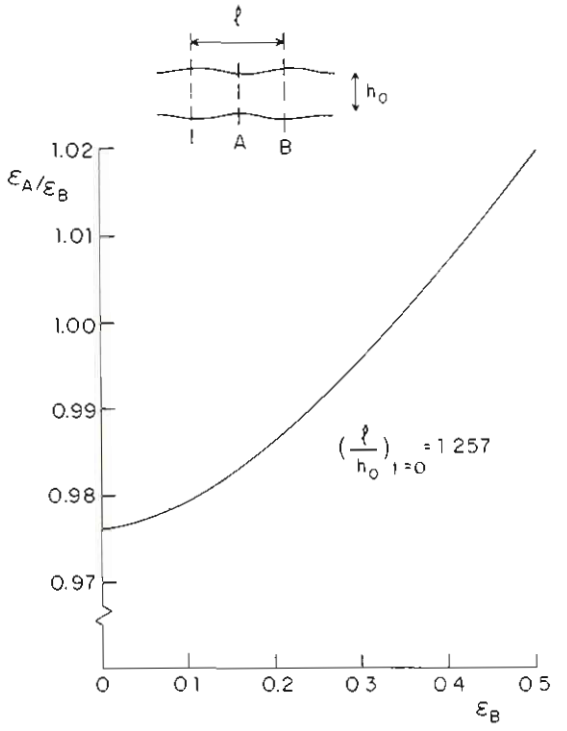

Fig. 5. Strains at the thinnest and thickest sections of the sheet for an initial wavelength to thickness ratio chosen to give an initial decrease in the relative size of the nonuniformity. (Initial amplitude $\xi = .01$; $n = 5$).

initial ratio of thicknesses at A and B is

$$h_A{}^0/h_B{}^0 = (1 - \xi)/(1 + \xi) = .980$$

The maximum strain attained at B according to the long-wavelength approximation is given by (56) with $\epsilon_A \to \infty$, i.e.,

$$\epsilon_B{}^* = -(1/n)\ln[1 - (h_A{}^0/h_B{}^0)^n] = .470 \tag{57}$$

Finite element results in Fig. 4 are shown for initial wavelength to thickness ratios of

$$(l/h_0)_{t=0} = 3 \quad \text{and} \quad 10$$

For these curves ϵ_A and ϵ_B are the effective strains at the minimum and maximum sections defined in terms of the respective current and initial thicknesses according to (55). (The variation of the strain-rates across the thickness direction at these sections is nearly constant for $n = 5$ as will be seen below.) From the exact results of the linearized analysis in Fig. 2 it can be seen that $G \cong .6$ for $l/h_0 = 3$ which, from (16), corresponds to an initial growth-rate which is sixty percent of the long-wavelength growth-rate. For $l/h_0 = 10$, $G \approx .92$ so that the initial growth-rate is much closer to the long-wavelength prediction. For an initial ratio

References p. 126.

$l/h_0 = 3$ the long-wavelength estimate for the limit strain ϵ_B^* falls below the actual value by more than 25 percent.

For the example in Fig. 5, $\xi = .01$, $n = 5$ with the initial ratio $l/h_0 = \pi/2.5 = 1.257$. From Fig. 2, $G \cong -.23$ and thus we expect the relative size of the nonuniformity to decrease initially. This is reflected in the finite element results in Fig. 5 by the fact that the ratio ϵ_A/ϵ_B is less than unity until ϵ_B reaches about .35. Once the current wavelength to thickness ratio l/h reaches about 1.8 the linearized analysis of Fig. 2 indicates that the relative size of the nonuniformity will begin to grow. Note, however, that even at $\epsilon_B = .5$ exceedingly little nonuniformity has developed compared to responses in Fig. 4.

Distributions of $\dot{\epsilon}_{11}/\dot{\epsilon}$ across the minimum section of the neck are shown for several values of n in Fig. 6, where $\dot{\epsilon}$ is the long-wavelength value (21). The dashed line curves are computed from the long-wavelength approximation with the lowest order h/R correction (50), while the solid line curves are from the finite element calculations. For each of the n-values in these figures the current thickness was taken to be the sinusoidal variation (7) with $l/h_0 = 3$. In Fig. 6(a),

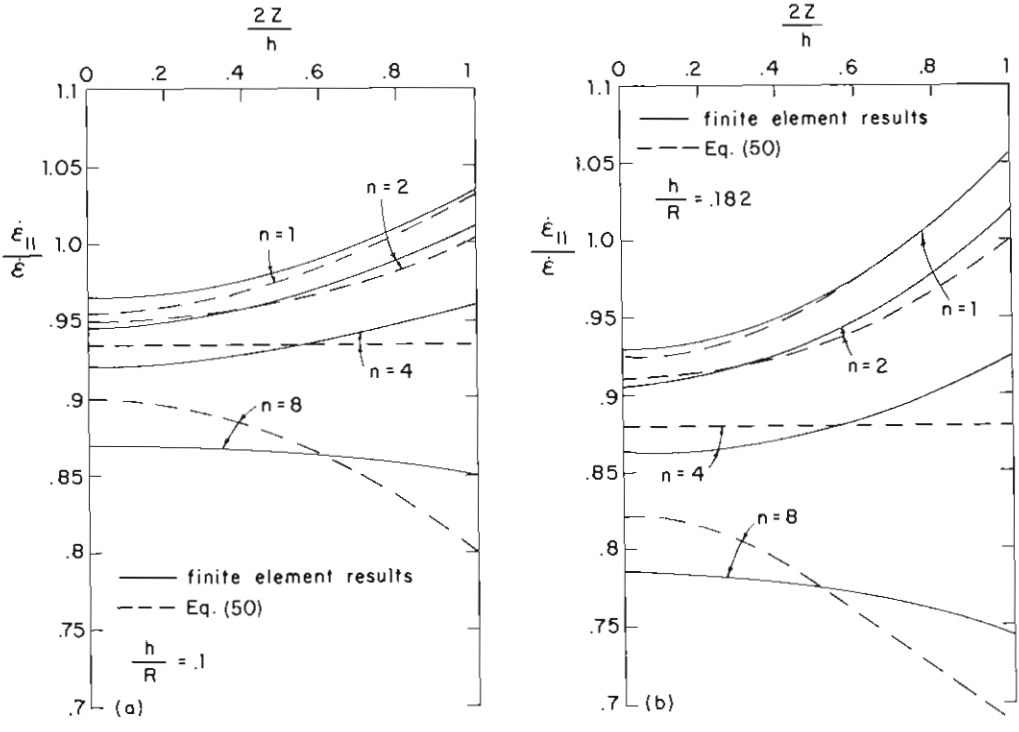

Fig. 6. Strain-rate distribution across the minimum section of the sheet—a comparison of the finite element results with the long-wavelength result including the lowest order correction given by equation (50). $\dot{\epsilon}$ is the long-wavelength result from equation (21). In (a), $l/h_0 = 3$ and $\xi = .048$ corresponding to $h/R = .1$; in (b), $l/h_0 = 3$ and $\xi = .0912$ corresponding to $h/R = .182$.

$\xi = .048$ corresponding to

$$h/R = 2\pi^2\xi(1 - \xi)(h_0/l)^2 = .1 \tag{58}$$

In Fig. 6(b), $\xi = .0912$ corresponding to $h/R = .182$. The larger is n, the larger is the order h/R correction term in (50). For $n = 8$ this correction term appears to be too large for the perturbation expansion, to order h/R, to retain accuracy in the present examples. For $n = 4$ the numerical results do show that $\dot{\epsilon}_{11}$ is approximately uniform across the neck. Even for $n = 8$, the strain-rate at the midsurface is reasonably approximated by (50).

DISCUSSION

The linearized analysis described in this paper reveals that, regardless of how *small* the amplitude of the thickness variation is, the growth-rate of the nonuniformity will be less than the prediction of the long-wavelength approximation if its wavelength is less than about four times the thickness. The perturbation analysis, on the other hand, complements the linearized analysis by showing that, regardless of how *large* the amplitude is, the long-wavelength approximation is valid if the wavelength of the variation is sufficiently large. At the neck minimum, h/R measures the extent to which departure from the long-wavelength approximation can be expected. If it is assumed that the current wavelength of the nonuniformity is sufficiently large so that the long-wavelength approximation is currently valid, it is a simple matter to calculate $(h/R)^{\cdot}$ at the neck minimum for the power law material (3). The result is

$$(h/R)^{\cdot} = (n - 2)\dot{\epsilon}h/R \tag{59}$$

in terms of the instantaneous quantities at the neck. Thus, if $n < 2$ and if the nonuniformity initially has a long-wavelength, then "localization" will not occur, since h/R decreases, and the long-wavelength analysis will actually become increasingly accurate. (The sheet will nevertheless shrink down to zero thickness at the minimum section with a finite limit strain at any other section of the form (57).) On the other hand, if $n > 2$, h/R increases and the stresses and strain-rates will progressively depart from the predictions of the long-wavelength analysis.

It is interesting to note that a slightly different criterion for localization based on steepening of the surface also leads to $n = 2$ as the transition point. Steepening of the neck surface depends on the convected rate of its slope, $(dh/dx_1)^{\cdot}$. Another relatively simple calculation, assuming the long-wavelength approximation applies, gives

$$(dh/dx_1)^{\cdot} = (n - 2)\dot{\epsilon}(dh/dx_1) \tag{60}$$

at an inflection point where $d^2h/dx_1^2 = 0$. Thus for $n < 2$ the magnitude of the slope at an inflection point decreases, while for $n > 2$ it steepens.

Localization in the above sense invariably leads to a breakdown of the long-wavelength approximation, as just discussed. Nevertheless, the major portion of the lifetime, in terms of straining outside the neck, may still be adequately

References p. 126.

represented by the long-wavelength approximation if the initial wavelength of the nonuniformity is sufficiently large, as is illustrated by the example of Fig. 4. This is an important consideration in our use of this approximation in Parts II and III where we will primarily be concerned with the amount of straining which can be attained in portions of the sheet away from the neck.

ACKNOWLEDGMENT

The work of J.W.H. was supported in part by the Air Force Office of Scientific Research under Grant AFOSR 77-3330, the National Science Foundation under Grant ENG76-04019, and by the Division of Applied Sciences, Harvard University. The work was conducted while K.W.N. was on leave at Harvard University. The support of the Faculty of Applied Sciences at the University of Sherbrooke is gratefully acknowledged. The work of A.N. was supported by the Materials Research Laboratory at Brown University funded by the National Science Foundation.

REFERENCES

[1] Z. Marciniak, K. Kuczyński, Int. J. Mech. Sci., *9* (1967), 609.
[2] J. W. Hutchinson and H. Obrecht, Fracture 1977, ICF4 (ed. D. M. R. Taplin), *1* (1977), 101.
[3] J. W. Hutchinson and K. W. Neale, Acta Met., *25* (1977), 839.
[4] E. J. Appleby and O. Richmond, to be published.
[5] P. W. Bridgman, Studies in Large Plastic Flow and Fracture, Harvard University Press (1964).
[6] A. Needleman and C. F. Shih, to be published.